Transient Three-dimensional Numerical Analysis of Forced Convection Flow and Heat Transfer in a Curved Pipe

Lect. Dr. Wajeeh Kamal Hasan
Refrigeration and Air Conditioning Engineering Department, Al-Rafidain University Collage, Iraq

Abstract: *A three-dimensional transient numerical study of a constant property Newtonian fluid in curved pipe under laminar flow conditions is presented for a uniform wall temperature boundary condition. Numerical solutions were obtained using the control volume method described by Patankar for the range of $(100 \leq Re \leq 200)$. The working fluid was water. The transient flow pattern and the temperature distribution on the tube section were derived for different values of the Reynolds number. Graphical results for velocity and temperature are presented and analyzed. Results have shown that the maximum velocity in center of velocity profile increase with increasing of Reynolds number. In curved pipes, time averaged results exhibited Dean circulation and a strong velocity and temperature stratification in the radial direction. Flow and heat transfer were strongly asymmetric, with higher values near the outer pipe bend.*

Keywords: *curved pipe, forced convection, internal flow, laminar flow, transient heat transfer*

Nomenclature

c_p Specific heat capacity (J. kg^{-1}. k^{-1})
De   Dean number
k   thermal conductivity (W. m^{-1}. k^{-1})
p   pressure (N . m^{-2})
r   radial coordinate
R   curvature radius of pipe (m)
Re   Reynolds number
T   temperature (K)
t   time (sec.)
v   velocity (m .s^{-1})
z   axial coordinate
Greek letters
θ   angular coordinate
ρ   density (kg.m^{-3})
Subscripts
i   internal
r   radial direction
z   axial direction
θ   tangential direction

I. Introduction

Interest in the problem of heat transfer in fully developed pipe flows dates back over a hundred years. The forced convection problems in curved pipes are frequently encountered in various heat exchanges, cooling or heating systems, chemical reactors, heat engines and other apparatus, equipment and devices. It is well known that the mode of fluid in a curved pipe is characterized by a secondary flow field, which is superimposed upon the axial-velocity flow field. The nature of the viscous flow in a curved pipe, as compared with simple straight-pipe parabolic flow, causes relatively high average heat- and mass-transfer rates per unit axial pressure drop, especially for fluid with a high Prandtl number and high Schmidt number. Of fundamental interest to the development of a complete understanding of viscous-flow phenomena in toroidal tubes is the nature of the velocity and temperature distributions in the fully-developed flow region.

As regards Flow field and pressure drop, in curved pipes a characteristic secondary motion develops in the cross section due to the imbalance between pressure and inertial (centrifugal) forces [1]. The fluid moves towards the outer bend side near the equatorial midplane, returns towards the inner side along two near-wall boundary layers, and then forms two symmetric secondary cells (Dean vortices) having a characteristic velocity scale $u_{av}\sqrt{\delta}$. The most popular friction correlations for curved pipes are those by Ito [4]:

$$f = \frac{64}{Re} \times \frac{21.5 \times De}{(1.56 + log_{10}De)^{5.73}} \qquad \text{(laminar flow)} \qquad (1)$$

$$f = 0.304 \times Re^{-0.25} + 0.029\sqrt{\delta} \qquad \text{(turbulent flow)} \qquad (2)$$

in which f is the Darcy friction coefficient (four times the Fanning friction coefficient) and Re is the bulk Reynolds number. Although its correlations date back to the 1950s, they have been confirmed to a very high degree of approximation by recent computational [2] and experimental [5] studies. Several authors attempted to characterize the transition to turbulence in curved pipes on the basis of friction coefficient measurements [5], flow visualization [6] or local flow/temperature measurements [7]. The main result of these studies is that curvature delays transition to turbulence with respect to straight pipes. For example, Srinivasan et al. [8] proposed the following correlation for the critical Reynolds number:

$$Re_{cr} = 2.1 \times 10^{3}\left(1 + 12\sqrt{\delta}\right) \qquad (3)$$

This exhibits the correct asymptotic behavior for d = 0 and predicts, for example, Re_{cr} = 10068 for δ = 0.1 and Re_{cr} = 15902 for δ = 0.3, values considerably higher than that (Re_{cr} = 2100) applicable to straight pipes. Among computational studies, Di Piazza and Ciofalo [2] presented detailed results on the breakdown of steady laminar flow and the transition to turbulence in closed toroidal pipes having curvatures δ of 0.1 and 0.3. They found periodic and quasi-periodic flow regimes, characterized by traveling waves, in a relatively narrow interval of Reynolds numbers and a rich scenario of transitions and bifurcations, including super- and sub-critical Hopf bifurcations and double Hopf bifurcations. Chaotic flow was obtained only for Re = 8000. Friedrich and co-workers [9, 10] presented numerical simulation results for toroidal and helical pipes at Re = 5600 (Re_{τ} = 230) and δ = 0.1. The authors performed a statistical processing of the solution (e.g. by computing Reynolds stresses), but the case they studied was a time-dependent laminar flow rather than a truly turbulent flow [2]. Moreover, only a tract of pipe 7.5 diameters long was modeled, using periodic boundary conditions at the ends; such conditions are inadequate for a truly predictive simulation of traveling waves since they force the wave length to be an exact sub-multiple of the arbitrary domain length. Similar remarks hold for the work of Webster and Humphrey [11], who presented flow visualizations and numerical simulations for curved pipes. The length of the computational domain was chosen to be equal to the wavelength that was experimentally measured. When the experiments evidenced traveling wave instability, the corresponding computational results showed oscillating velocities with maximum rms values in the Dean Vortex region. A quantitative comparison with experiments was not possible since these latter were limited to flow visualization. As regards heat transfer, many experimental studies were performed in the 1960s and the 1970s on the average heat transfer rate in curved and helical pipes, e.g. by Seban and McLaughlin [12] and Mori and Nakayama [13]; only some of these investigations explored the influence of the Prandtl number on heat transfer, and very few investigated the local heat transfer rate distribution. The results of most of such studies will not be reported here and will not be used for validation purposes because they are either insufficiently confirmed, or limited to a range of parameters too far from that of interest here; the reader is referred to the recent reviews presented by Naphon and Wongwises [14] and by Vashist et al. [15]. Rogers and Mayhew [16] proposed for the Nusselt number in helical pipes the following power-law correlation:

$$Nu = 0.023Re^{0.85}Pr^{0.4}\delta^{0.1} \qquad (4)$$

This formula basically is a curvature correction to the Dittus–Bolter correlation; since it does not contain the pipe torsion, it does not distinguish between planar and helical curved pipes. Unfortunately, Eq. (4) does not exhibit the correct asymptotic behavior for small δ, predicting Nu = 0 for straight pipes.

Xin and Ebadian [17] presented an experimental study on heat transfer in helical pipes; the authors explored two values of curvature, i.e., δ = 0.027 and 0.08, Re from 5 x 10^3 to 1.1 x 10^5, and three different fluids, i.e., air (Pr = 0.7), water (Pr = 5), and ethylene glycol (Pr = 175), covering a broad range of Prandtl numbers. Results for air and water (0.7 < Pr < 5) were approximated by the following correlation:

$$Nu = 0.00619\ Re^{0.92}\ Pr^{0.4}(1 + 3.455\delta) \qquad (5)$$

with an RMS deviation of 18% for 0.7 < Pr < 5.5 x 10^3 < Re < 10^5, 0.0267 < δ < 0.0884. Eq. (5), like Eq. (4), does not distinguish between planar and helical pipes; unlike Eq. (4), it offers a reasonable asymptotic behavior for straight pipes, but is strictly applicable only to the narrow curvature range of the experiments. As regards computational studies on heat transfer in curved pipes, they are relatively numerous, but most of them regard laminar flow or geometrical configurations much different from those discussed in the present paper. Some authors concentrated on the simulation of the shell-side heat transfer in heat exchangers with helically coiled tubes [18,19] or considered helical coils just as components of the larger system represented by the heat exchanger or steam generator [20,21]. Litster et al. [22] studied laminar mass transfer in helical pipes using the CFX4.3 finite volume code. Bolinder and Sundèn [23] computed laminar heat transfer in helical coils of square cross section. Centrifugal and gravitational buoyancy in laminar flow was the focus of several studies [24–27]. Yang et al. [28] studied laminar flows in serpentine pipes, in which the pipe axis lies in a plane but left- and

right-turn bends alternate periodically. Other studies are dedicated to the possible mixing effects of chaotic advection even in the presence of steady laminar flow, especially when coils with three-dimensionally alternating axes are used [29,30].

The purpose of this work is to investigate numerically the transient three-dimensional laminar flow heat transfer in a 135° curved circular pipe under the thermal boundary conditions of constant wall temperature. At the inlet of the curved pipe, a parabolic velocity profile is imposed. Water is used as the working fluid. The effects of governing non-dimensional parameters, such as Reynolds number, *Re*, on the flow characteristics involving axial flow, secondary flow pattern and temperature profiles are investigated in details.

II.   Description of the Physical Problem

The geometry and characteristics of the curved pipe used in the present study are shown in Fig.1. The inner diameter of the pipe is 0.01 m and the outer 0.012 m, respectively. It is bending to a 135° angle with a radius of 0.02 m. beyond the bend, 0.03 m of the direct part is also accounted for.

III.   Mathematical Model

The transient laminar flow (20 < De < 1200) in the curved pipe is considered. All the thermo- physical properties are assumed to be constant. Water is considered to be an incompressible Newtonian fluid. Viscous dissipation and body force are considered to be negligibly small and dropped from the energy and momentum equations respectively. The extra body force due to curvature is considered in the momentum equation. Coordinate system is shown in Figure 1. In this system, the radius of curvature of the pipe axis is shown by R. The distance along the pipe axis is shown by z, the distance in the radial direction measured from the pipe axis by r. The velocity components in the directions of increasing r, θ, z are v_r, v_θ, v_z, respectively. On the basis of the simplifying assumptions, the transient three-dimensional governing equations are summarized as follows:

The equation of continuity: $\frac{\partial v_r}{\partial r} + \frac{1}{r}\frac{\partial v_\theta}{\partial \theta} + \frac{\partial v_z}{\partial z} + \frac{v_r}{r} = 0$ (6)

The equations of Motion (momentum equation):

$$\rho\left(\frac{Dv_r}{Dt} - \frac{v_\theta^2}{r}\right) = -\frac{\partial p}{\partial r} + \mu\left(\nabla^2 v_r - \frac{v_r}{r^2} - \frac{2}{r^2}\frac{\partial v_\theta}{\partial \theta}\right) + \frac{\rho v_z^2}{R}\cos\theta \qquad \text{(7-a)}$$

$$\rho\left(\frac{Dv_\theta}{Dt} + \frac{v_r v_\theta}{r}\right) = -\frac{1}{r}\frac{\partial p}{\partial \theta} + \mu\left(\nabla^2 v_\theta + \frac{2}{r^2}\frac{\partial v_r}{\partial \theta} - \frac{v_\theta}{r}\right) - \frac{\rho v_z^2}{R}\sin\theta \qquad \text{(7-b)}$$

$$\rho\frac{Dv_z}{Dt} = -\frac{\partial p}{\partial z} + \mu\nabla^2 v_z \qquad \text{(7-c)}$$

Where: $\frac{D}{Dt} = \frac{\partial}{\partial t} + v_r\frac{\partial}{\partial r} + \frac{v_\theta}{r}\frac{\partial}{\partial \theta} + v_z\frac{\partial}{\partial z}$ (8)

The energy equation:

$$k\left[\frac{1}{r}\frac{\partial}{\partial r}\left(r\frac{\partial T}{\partial r}\right) + \frac{1}{r^2}\frac{\partial^2 T}{\partial \theta^2} + \frac{\partial^2 T}{\partial z^2}\right] = \rho c_p\frac{\partial T}{\partial t} + \rho c_p\left(v_r\frac{\partial T}{\partial r} + \frac{v_\theta}{r}\frac{\partial T}{\partial \theta} + v_z\frac{\partial T}{\partial z}\right) \qquad \text{(9)}$$

3.1 Boundary and Initial Conditions:

The governing equations of the fluid flow are non-linear and coupled partial differential equations, subjected to the following boundary conditions. At the inlet of the curved pipe, a parabolic velocity profile is imposed. This eliminates the hydrodynamic entrance length required to obtain a fully developed velocity profile before heating begins. The temperature of the water is set equal to 350 K at the inlet of the computational domain. Standard no slip boundary condition was used on the walls of the curved pipe. A constant wall temperature boundary condition was imposed on the external walls of curved pipe. The walls of the curved pipe are kept at 300 K. Outflow boundary conditions were enforced for the outlet section. This boundary condition implies zero normal gradients for all flow variables except pressure. At the initial state, the water velocity, vr = v_θ = v_z = 0, everywhere, water temperature, T= 0, instantly, they are changed from the initial state to the inlet conditions.
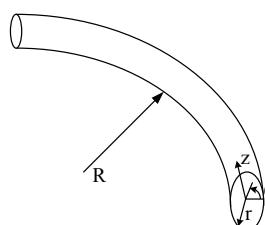

fig. (1): Geometry and coordinate system

3.2 Numerical Procedure

A mathematical model, i.e. differential equations, with initial and boundary conditions, has been discretised using the control volume method described by Patankar [31]. The velocities and pressure of heat transfer fluid are solved by using the SIMPLER scheme [31]. The resulting discretisation equations have been solved simultaneously using Biconjugate Gradient Stabilized iterative procedure. Due to nonlinearity of the problem, iterations are needed during each time step. The first order time derivatives are discretized using the second order Backward Differences Formulae time-stepping method. A convergence criterion is set at 1.0e-10 for all variables of the system. In order to improve convergence, under relaxation factors were used both for the velocity components and temperature. Typical values used from 0.2 - 1.0.

IV. Results and Discussion

The numerical computations were carried out for the curved pipe. The forced convection heat transfer in curved pipe was investigated under laminar flow conditions. The Reynolds number Re was varied in the range of 100 to 200. The parametric study conducted produced a large number of results. In order to present some characteristic velocity and isotherm contours, some samples of results are chosen as shown below. Figs. (3a, 5a, and 7a) show the typical velocity magnitude contours on a section along (r-z) plane while Figs. (3b, 5b, and 7b) show the contours of velocity at the outlet plane of the pipe for different Reynolds numbers. These velocity contours provide information on the effect of Reynolds numbers on the flow field. The typical temperature contours predicted by the present numerical computations for flow in the pipe on a section along (r-z) plane are shown in Figs. (2a, 4a, and 6a) and Figs. (2b, 4b, and 6b) show these contours at the outlet plane of the pipe for different Reynolds numbers. An inspection of these figures reveals the effect of Reynolds numbers on the heat transfer. A close study of these figures indicates that the centrifugal body forces induced by the wall curvature have a strong influence on the heat transfer. At low Reynolds numbers the centrifugal body forces are weaker and the convective currents have strong influence on the flow. The velocity profile presents the characteristic parabolic shape. At higher Reynolds numbers the centrifugal body forces are now much stronger and the secondary flow motion begins to show its effect on flow and heat transfer. The distortion of the velocity profile is not negligible. As a consequence, also the temperature profile is distorted showing an increase of the gradients at the wall. There are stronger temperature gradients on the convex surface of the pipe. In other words, the convex surface of the pipe influences heat transfer more than the concave surface of the pipe. Figs. (3b, 5b and 7b) reveal that the flow development is symmetric about the horizontal pipe centerline.

At the low Reynolds numbers depending on the curvature, the maximum axial velocity stays on the semi-inner portion of the curved pipe where the viscous forces dominate to the centrifugal forces generated due to the curvature of the curved pipe. When the centrifugal forces dominate to viscous forces, typically at higher Reynolds numbers, the maximum axial velocity covers the semi-outer portion of the curved. As the Reynolds number increases, the Dean vortices generated due to centrifugal forces at the outer and inner curved walls of the pipe become stronger and depending on the Reynolds number they break into two or more small vortices. Transient temperature and velocity distributions obtained by numerical calculation are also shown in these figures for different time periods. Contours of temperatures for different time periods are shown in Figs. (2, 4 and 6). These figures indicate that heat transfer during the initial transient period is primarily governed by the radial conduction mechanism, and heat transfer by axial convection and conduction effects increases with time. As the time increase, temperature fluctuations are small, interest a thin near-wall region, and are azimuthally non-uniform, being more intense in the outer bend region.

the velocity's contours for different time periods are also shown in Figs. (3, 5 and 7).with a parabolic inlet velocity, the fluid particles close to the center of curvature have larger centrifugal forces than the others near the inlet, and they tend to push the fluid far away from the center of curvature and the secondary velocities are much less intense and tend to concentrate near the outer bend region as the time increase. also, from these figures, we can observes that ,with increasing time, one pair of vortices appeared to grow up due to the high radial pressure gradient and substantial tendency of the main flow toward outer wall which lead the flow to be changed.
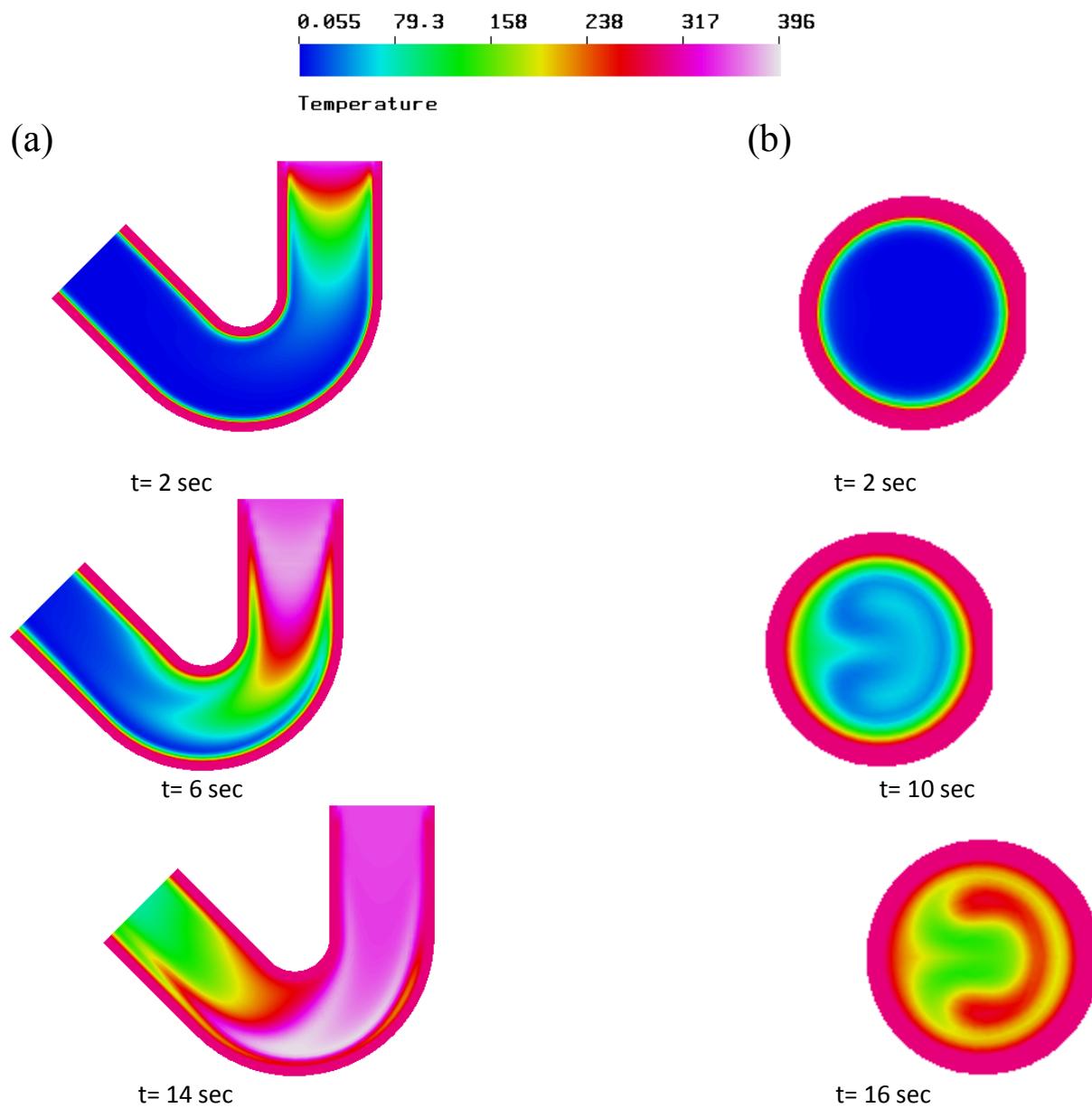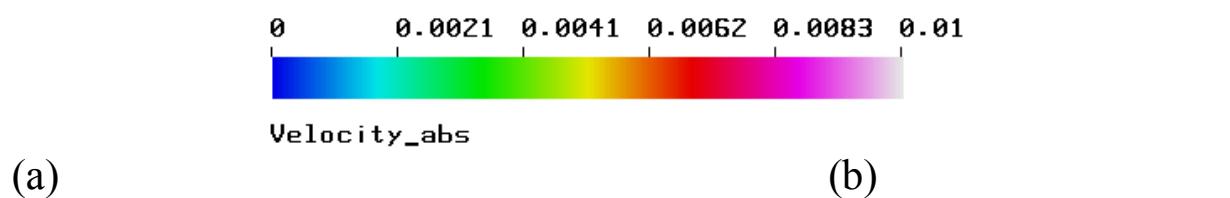
fig.(2): contours of temperature of the pipe's fluid for different time periods, Re=100, on a section along: (a) r-z plane , (b) r-θ plane
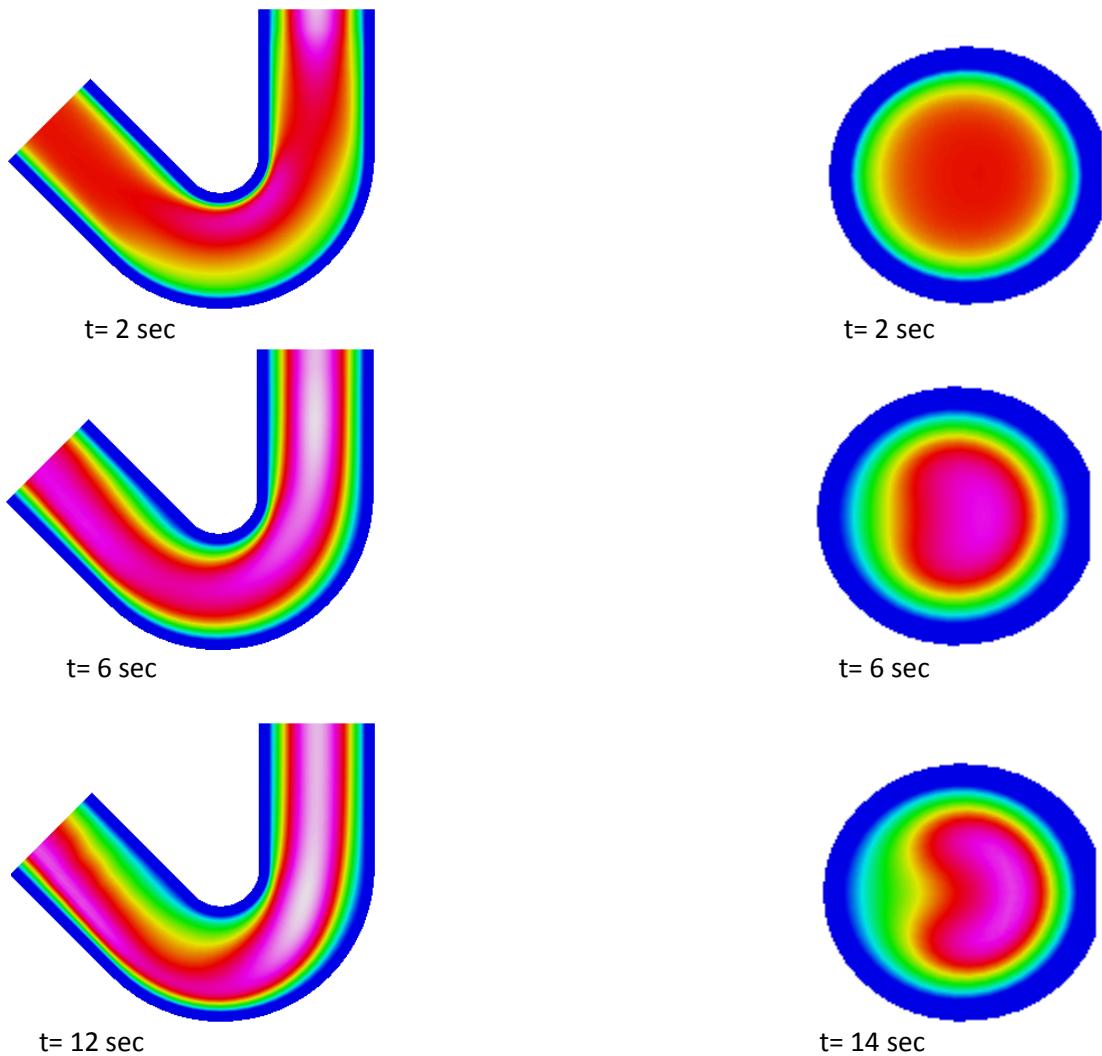
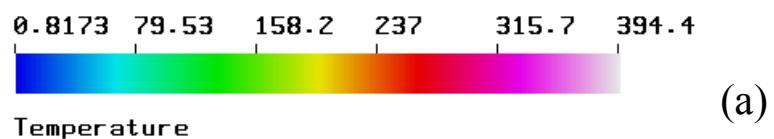fig.(3): velocity contours of the pipe's fluid for different time periods, Re=100, on a   section
along: (a) r-z plane , (b) r-θ plane

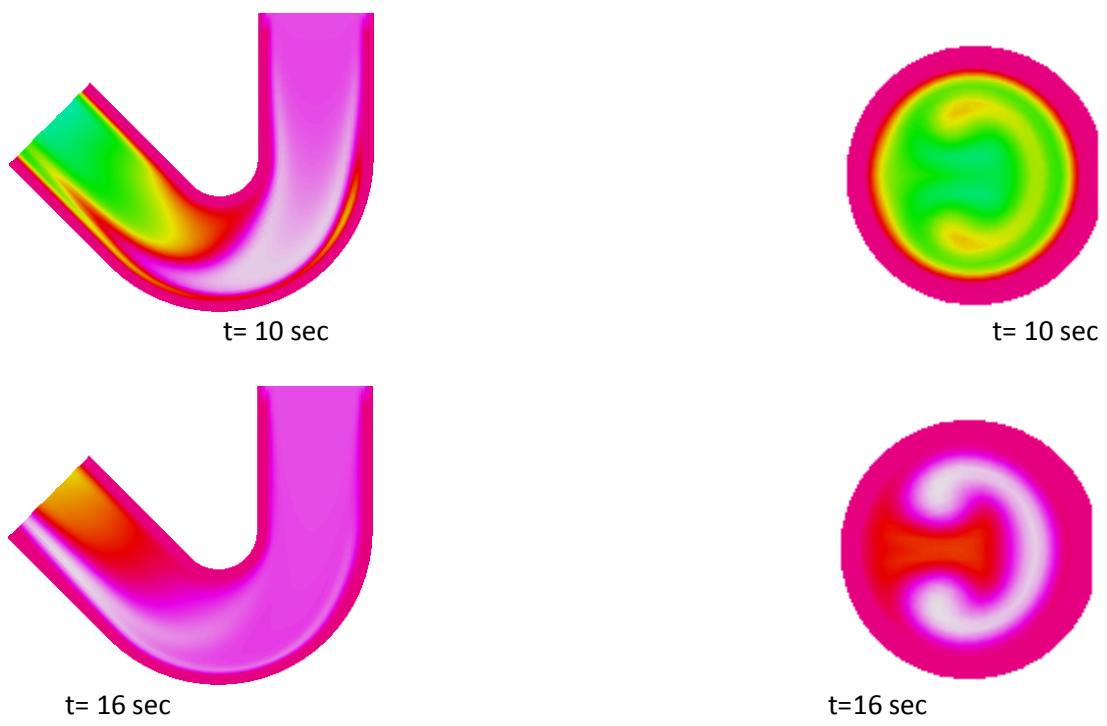t= 10 sec

t= 10 sec

t= 16 sec

t=16 sec

fig.(4): contours of temperature of the pipe's fluid for different time periods, Re=150, on a section along: (a) r-z plane , (b) r-θ plane

0   0.0031   0.0062   0.0093   0.012   0.016

Velocity_abs

(a)

(b)

t= 2 sec
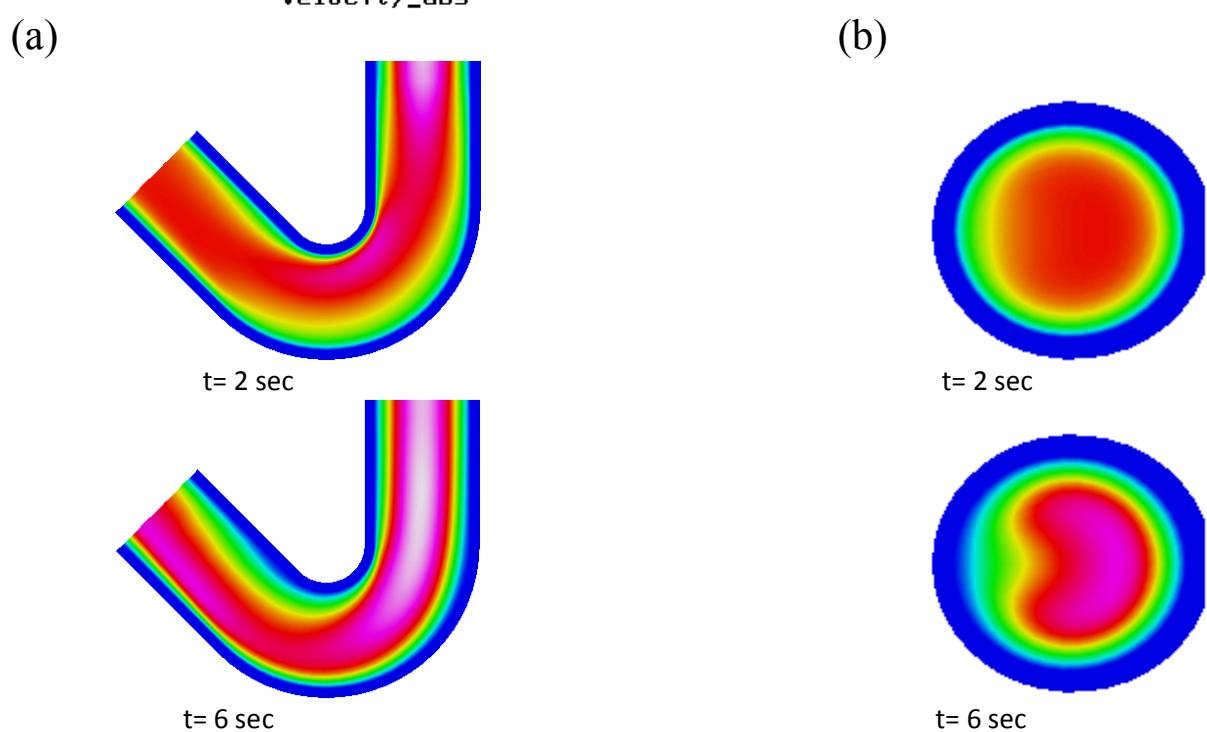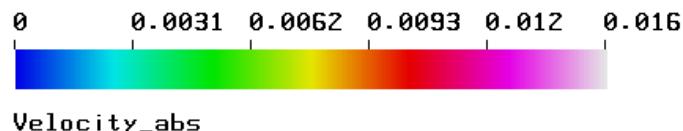
t= 2 sec

t= 6 sec

t= 6 sec

t= 12 sec

t= 14 sec

fig.(5): velocity contours of the pipe's fluid for different time periods, Re=150, on a   section along: (a) r-z plane , (b) r-θ plane
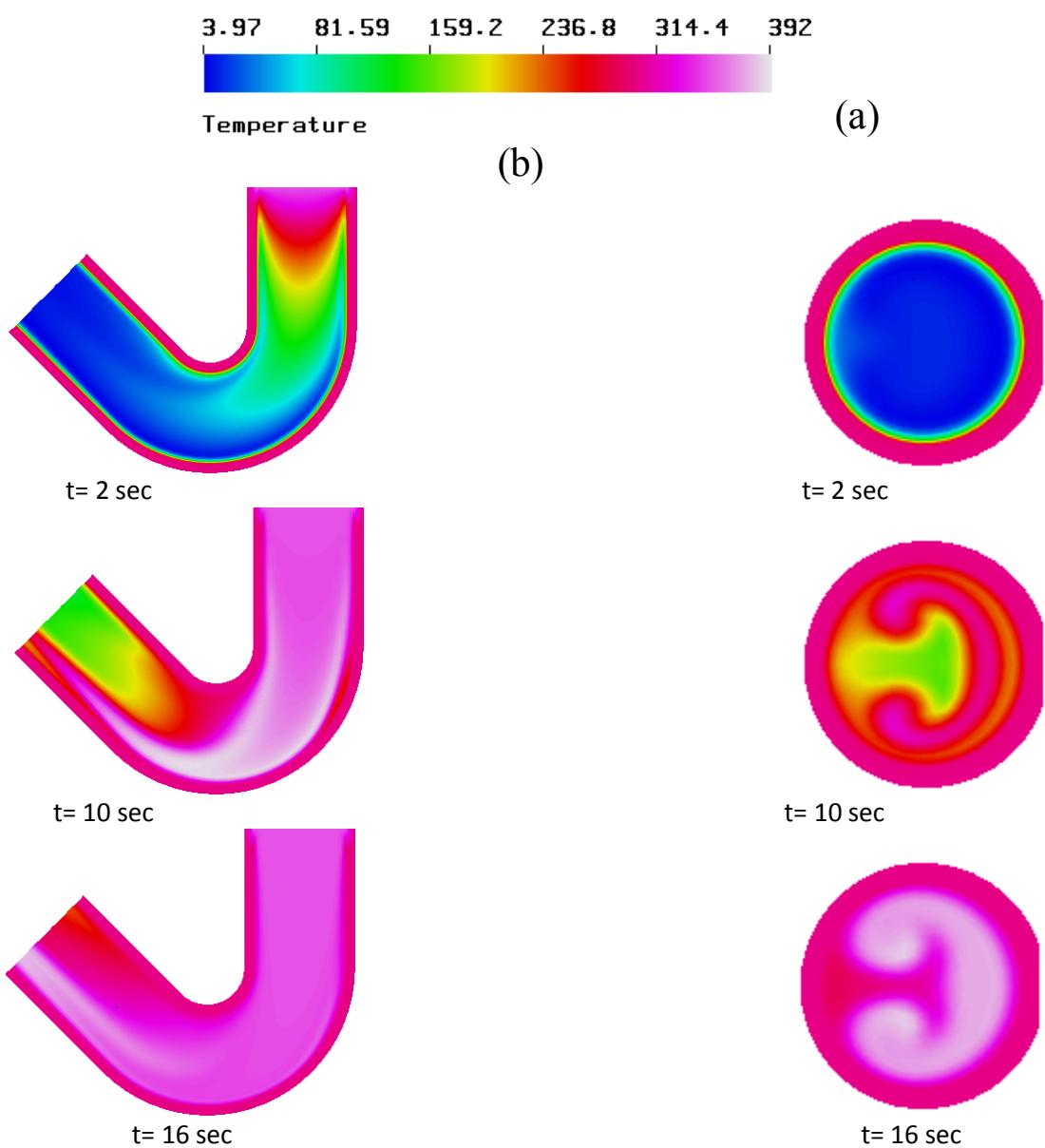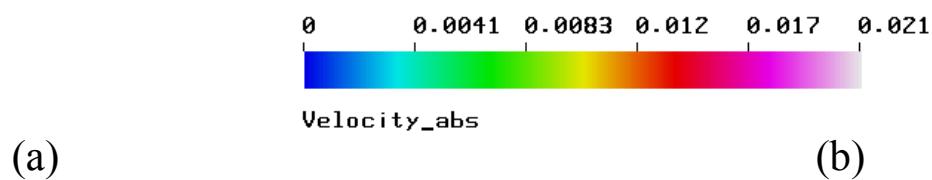

t= 2 sec

t= 2 sec

t= 10 sec

t= 10 sec

t= 16 sec

t= 16 sec

fig.(6): contours of temperature of the pipe's fluid for different time periods, Re=200, on a section along: (a) r-z plane , (b) r-θ plane

0   0.0041 0.0083 0.012   0.017   0.021

Velocity_abs

(a)   (b)

t= 2 sec

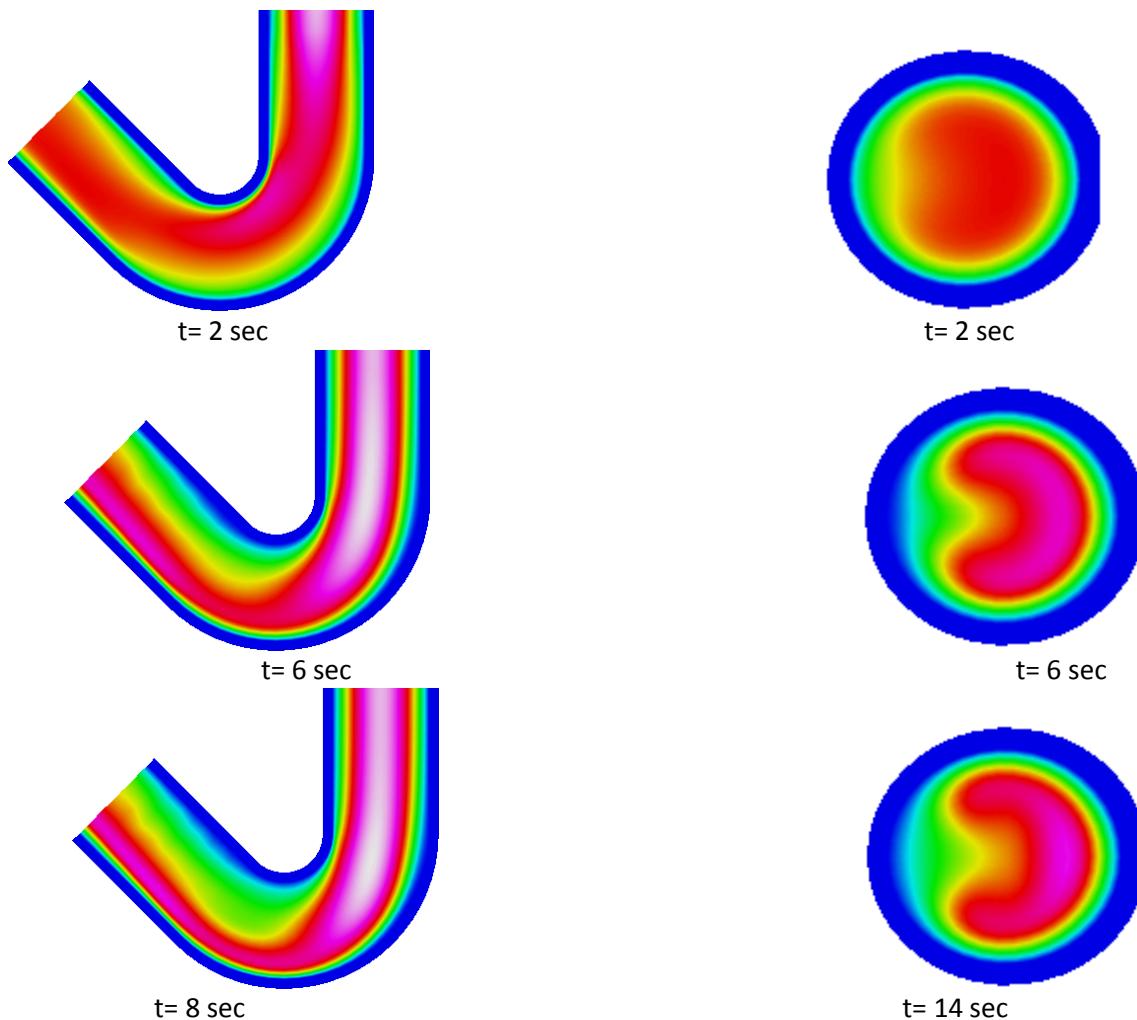t= 2 sec

t= 6 sec

t= 6 sec

t= 8 sec

t= 14 sec

fig.(7): velocity contours of the pipe's fluid for different time periods, Re=200, on a   section along: (a) r-z plane , (b) r-θ plane

V. Conclusions

A numerical model was developed to predict the transient flow and heat transfer behavior of water throughout a curved pipe. Laminar forced convection heat transfer with constant wall temperature has been investigated. Simultaneous effects of the centrifugal forces have been shown. The effects of the Reynolds number on velocity and temperature are presented. The results of numerical analysis show that when the inlet temperature is suddenly changed from the initial temperature, conduction in the radial direction is the governing heat transfer mechanism at the initial transient period, but as time passes, axial convection and conduction effects are relatively increased and become an important heat transfer after a certain time. In curved pipes, results showed the presence of secondary (Dean) circulation and of a strong stratification of stream wise velocity and temperature along the radius of curvature. At the low Reynolds numbers, the maximum axial velocity stays on the semi-inner portion of the curved pipe. When the centrifugal forces dominate to viscous forces, typically at higher Reynolds numbers, the maximum axial velocity covers the semi-outer portion of the curved and the Dean vortices generated due to centrifugal forces at the outer and inner curved walls of the pipe become stronger and they break into two or more small vortices.

References

[1]   S.A. Berger, L. Talbot, L.S. Yao, Flow in curved pipes, *Ann. Rev. Fluid Mech., 15*, 1983, 461–512.
[2]   I. Di Piazza, M. Ciofalo, Transition to turbulence in toroidal pipes, *J. Fluid Mech., 687* , 2011, 72–117.
[3]   M. Germano, On the effect of torsion in a helical pipe flow, *J. Fluid Mech., 125*, 1982, 1–8.
[4]   H. Ito, Friction factors for turbulent flow in curved pipes, *J. Basic Eng., 81*, 1959, 123–134.
[5]   A. Cioncolini, L. Santini, An experimental investigation regarding the laminar to turbulent flow transition in helically coiled pipes, *Exp. Therm. Fluid Sci., 30*, 2006, 367–380.
[6]   R. Narasimha, K.R. Sreenivasan, Relaminarization of fluid flows, Adv. Appl. Mech. 19 (1979) 221–309.
[7]   K.R. Sreenivasan, P.J. Strykowski, Stabilization effects in flow through helically coiled pipes, *Exp. Fluids, 1*, 1983, 31–36.
[8]   S. Srinivasan, S. Nadapurkar, F.A. Holland, Friction factors for coils, *Trans. Inst. Chem. Eng., 48,* 1970, T156–T161.

[9] T.J. Hüttl, R. Friedrich, Direct numerical simulation of turbulent flows in curved and helically coiled pipes, *Comput. Fluids, 30,* 2001, 591–605.

[10] R. Friedrich, T.J. Hüttl, M. Manhart, C. Wagner, Direct numerical simulation of incompressible turbulent flows, *Comput. Fluids, 30*, 2001, 555–579.

[11] D.R. Webster, J.A.C. Humphrey, Travelling wave instability in helical coil flow, *Phys. Fluids, 9,* 1997, 407–418.

[12] R.A. Seban, E.F. McLaughlin, Heat transfer in tube coils with laminar and turbulent flow, *Int. J. Heat Mass Transfer, 6* , 1963, 387–395.

[13] Y. Mori, W. Nakayama, Study of forced convective heat transfer in curved pipes, *Int. J. Heat Mass Transfer, 11* , 1967, 37–59.

[14] P. Naphon, S. Wongwises, A review of flow and heat transfer characteristics in curved tubes, *Renew. Sustain. Energy Rev., 10,* 2006, 463–490.

[15] S. Vashisth, V. Kumar, D.P.K. Nigam, A review on the potential application of curved geometries in process industry, *Ind. Eng. Chem. Res., 47,* 2008, 3291– 3337.

[16] G.F.C. Rogers, Y.R. Mayhew, Heat transfer and pressure loss in helically coiled tubes with turbulent flow, *Int. J. Heat Mass Transfer, 7,* 1964, 1207–1216.

[17] R.C. Xin, M.A. Ebadian, The effects of Prandtl numbers on local and average convective heat transfer characteristics in helical pipes, *J. Heat Transfer, 119,* 1997, 467–473.

[18] J.S. Jayakumar, S.M. Mahajani, J.C. Mandal, P.K. Vijayan, R. Bohi, Experimental and CFD estimation of heat transfer in helically coiled heat exchangers, *Chem. Eng. Res. Des., 86*, 2008, 211–232.

[19] M.R. Salimpour, Heat transfer coefficients of shell and coiled tube heat exchangers, *Exp. Therm. Fluid Sci., 33,* 2009, 203–207.

[20] J.C. Ho, N.E. Wijeysundera, S. Rajasekar, T.T. Chandratilleke, Performance of a compact spiral coil heat exchanger, *Heat Recovery Syst. CHP, 15,* 1995, 457– 468.

[21] Y. Rabin, E. Corin, Thermal analysis of a helical heat exchanger for ground thermal energy storage in arid zones, *Int. J. Heat Mass Transfer, 39,* 1996, 1051–1065.

[22] S. Litster, J.G. Pharoah, N. Djilali, Convective mass transfer in helical pipes: effect of curvature and torsion, *Heat Mass Transfer, 42* , 2006, 387–397.

[23] C.J. Bolinder, B. Sundèn, Numerical prediction of laminar flow and forced convective heat transfer in a helical square duct with a finite pitch, *Int. J. Heat Mass Transfer, 39*, 1996, 3101–3115.

[24] D.J. Goering, J.A.C. Humphrey, R. Greif, The dual influence of curvature and buoyancy in fully developed tube flows, *Int. J. Heat Mass Transfer, 49,* 1997, 2187–2199.

[25] J.J.M. Sillekens, C.C.M. Rindt, A.A. van Steenhoven, Developing mixed convection in a coiled heat exchanger, *Int. J. Heat Mass Transfer, 41,* 1998, 61–72.

[26] T.W. Gyves, T.E. Irvine Jr., M.N.M. Naraghi, Gravitational and centrifugal buoyancy effects in curved square channels with conjugate boundary conditions, *Int. J. Therm. Sci., 42,* 1999, 2015–2029.

[27] H. Chen, B. Zhang, Fluid flow and mixed convection heat transfer in a rotating curved pipe, *Int. J. Therm. Sci., 42,* 2003, 1047–1059.

[28] R. Yang, S.F. Chang, W. Wu, Flow and heat transfer in curved pipe with periodically varying curvature, *Int. Commun. Heat Mass Transfer, 27* , 2000, 133–143.

[29] N. Acharya, M. Sen, H.-C. Chang, Analysis of heat transfer enhancement in coiled-tube heat exchangers, *Int. J. Heat Mass Transfer, 44,* 2001, 3189– 3199.

[30] T. Lemenand, H. Peerhossaini, A thermal model for prediction of the Nusselt number in a pipe with chaotic flow, *Appl. Therm. Eng., 22,* 2002, 1717–1730.

[31] Patankar, S. V.: *numerical heat transfer and fluid flow* (Hemisphere Publishing Corporation, Taylor & Francis Group, New York, 1980).